Alzheimer's & Dementia: Diagnosis, Assessment & Disease Monitoring 10 (2018) 471-479

Neuroimaging

Early affective changes and increased connectivity in preclinical Alzheimer's disease

Carolyn A. Fredericks[a,*], Virginia E. Sturm[a], Jesse A. Brown[a], Alice Y. Hua[a], Murat Bilgel[b], Dean F. Wong[c], Susan M. Resnick[b], William W. Seeley[a,d]

[a]*Memory and Aging Center, Department of Neurology, University of California, San Francisco, CA, USA*
[b]*Laboratory of Behavioral Neuroscience, National Institute on Aging, Baltimore, MD, USA*
[c]*Department of Radiology and Radiological Science, Johns Hopkins University, Baltimore, MD, USA*
[d]*Department of Pathology, University of California, San Francisco, CA, USA*

Abstract

Introduction: Affective changes precede cognitive decline in mild Alzheimer's disease and may relate to increased connectivity in a "salience network" attuned to emotionally significant stimuli. The trajectory of affective changes in preclinical Alzheimer's disease, and its relationship to this network, is unknown.

Methods: One hundred one cognitively normal older adults received longitudinal assessments of affective symptoms, then amyloid-PET. We hypothesized amyloid-positive individuals would show enhanced emotional reactivity associated with salience network connectivity. We tested whether increased global connectivity in key regions significantly related to affective changes.

Results: In participants later found to be amyloid positive, emotional reactivity increased with age, and interpersonal warmth declined in women. These individuals showed higher global connectivity within the right insula and superior temporal sulcus; higher superior temporal sulcus connectivity predicted increasing emotional reactivity and decreasing interpersonal warmth.

Conclusions: Affective changes should be considered an early preclinical feature of Alzheimer's disease. These changes may relate to higher functional connectivity in regions critical for social-emotional processing.

Keywords: Amyloid-PET; Alzheimer's disease; Preclinical Alzheimer's disease; Neuropsychiatric symptoms; Functional connectivity

1. Background

Patients with mild-to-moderate Alzheimer's disease (AD) often show strikingly preserved social sensitivity. They retain the emotional trace of film clips despite forgetting their narrative content [1], show preserved mutual gaze with their spouses [2], and have a heightened tendency to take on the emotions of those around them [3]. This sensitivity can have less desirable effects, manifesting as anxiety, irritability, and agitation, among the most common neuropsychological symptoms in early AD [4]. Differences in emotional reactivity may precede the onset of cognitive decline: increased midlife neuroticism, a trait indicator suggesting increased reactivity to negative emotion [5], is associated with higher rates of late-life AD [6]. Cognitively intact individuals with preclinical AD report more loneliness than their peers, independent of objective social network measures [7]. Whether differences in emotional reactivity and social experience represent a risk factor for AD or an early manifestation of AD pathological changes remains uncertain.

Amyloid-PET is increasingly accepted as a strong early predictor of future AD. A newly positive amyloid-PET scan predicts progression to AD dementia within 20–30

*Corresponding author. Tel.: 650 721 5357; Fax: 650 725 0390.
E-mail address: cfrederi@stanford.edu

https://doi.org/10.1016/j.dadm.2018.06.002

years, based on a recent large meta-analysis [8], and the National Institute on Aging and Alzheimer's Association workgroup defines the presence of a positive amyloid-PET scan in cognitively healthy individuals as the first stage of preclinical AD [9]. The functional neuroimaging literature suggests that AD and, more variably, preclinical AD defined by amyloid positivity are associated with decreased connectivity in the default mode network (DMN), which supports episodic memory [10–14]. AD is, conversely, associated with increases in connectivity, gray matter volume, and perfusion within a salience network, which responds to diverse stimuli of homeostatic relevance to the individual, including socioemotional cues [15–17]. Salience network connectivity correlates with emotional reactivity in AD [18]. The point at which salience network connectivity increases relative to the development of AD pathology remains uncertain, though cognitively healthy carriers of an apolipoprotein E (APOE) ε4 allele, the major genetic risk factor for late-onset AD, show widespread salience network connectivity increases [19].

In this study, we sought to determine whether salience network connectivity intensification and longitudinal increases in emotional reactivity could be detected in cognitively normal amyloid-positive individuals. We studied participants of the Baltimore Longitudinal Study of Aging (BLSA), a large longitudinal aging cohort with follow-up data spanning 2 decades [20]. We hypothesized that cognitively normal older individuals found to be amyloid positive would show a trajectory of increasing emotional reactivity but preserved to increased scores on measures of interpersonal warmth, both in absolute terms and relative to amyloid-negative peers. We further hypothesized that longitudinal increases in these measures would be associated with higher global connectivity within key salience network nodes, and that these associations would be present in the absence of significant atrophy.

2. Methods

2.1. Participants

Participants were volunteers in the BLSA, an ongoing cohort study of older community-dwelling adults. Each participant underwent an extensive evaluation, including personality and cognitive assessments, biennially for ages 60–79 years and annually for participants 80 years and older. Those selected for analysis had additionally undergone [^{11}C]-Pittsburgh compound B (PiB)–PET (n = 101) at the time of their most recent available study visit; of these, a subset had also undergone structural and task-free functional task-free functional magnetic resonance imaging (tf-fMRI) and were included in further analysis (Fig. 1). BLSA research protocols were approved by the institutional review boards of the National Institute on Aging and Johns Hopkins Medical Institutions; all participants provided written informed consent before each visit. Participants selected for analysis had undergone longitudinal personality assessments for a mean of 14.0 years (standard deviation 8.1 years) before the PiB-PET session and were free of cognitive impairment at the time of their PiB-PET and magnetic resonance imaging (MRI) sessions by clinical consensus based on review of clinical and neuropsychological assessments [21]. Between-group demographic variables were compared using Welch's t-test and χ^2 tests as appropriate.

2.2. Assessment of emotional reactivity and interpersonal warmth

Personality was assessed using the self-report version of the revised NEO Personality Inventory (NEO-PI-R), a widely used measure of the so-called "Big Five" personality traits (neuroticism, extraversion, openness to experience, agreeableness, and conscientiousness) for which population-based norms are available [22]. We calculated neuroticism and extraversion composites from NEO-PI-R subscales selected to best represent the individual's response to socially salient stimuli. These included a neuroticism composite (referred to henceforth as "emotional reactivity") based on NEO-PI-R subscales N1 (anxiety), N3 (depression), and N6 (vulnerability), and an extraversion composite (referred to henceforth as "interpersonal warmth") based on NEO-PI-R subscales E1 (warmth) and E6 (positive emotion). In addition to having face validity for the affective science constructs of interest, the subscales selected are the strongest loading variables within the neuroticism and extraversion facets; that is, of the available subscales, they are the most central to neuroticism and extraversion [23]. Composites represented sums of each subject's t scores (drawn from large sample norms, with mean = 50 and standard deviation = 10) for each measure to ensure a common metric across measures. Analyses included all available NEO assessments before and concurrent with PiB-PET.

2.3. Image acquisition

Participants underwent [^{11}C] PiB-PET, conducted on a GE Advance scanner (GE Medical Systems, Milwaukee, WI). For subjects with more than one session of PiB-PET available, we used the scanning session closest to the latest available NEO assessment. 3D dynamic PiB-PET data acquisition was performed immediately following an intravenous bolus injection of approximately 15-mCi [^{11}C] PiB with an acquisition protocol of 4 × 0.25, 8 × 0.5, 9 × 1, 2 × 3, 10 × 5 minutes (total 70 min, 33 frames). Images were corrected for attenuation using ^{68}Ge transmission scans and reconstructed using filtered back-projection with a ramp filter, yielding a spatial resolution of approximately 4.5-mm full width at half max at the center of the field of view. Pixel size and slice thickness of the resulting images were 2 × 2 mm^2 and 4.25 mm, respectively.

A subset of individuals from the NEO-PiB data set additionally underwent tf-fMRI using a 3T Philips Achieva

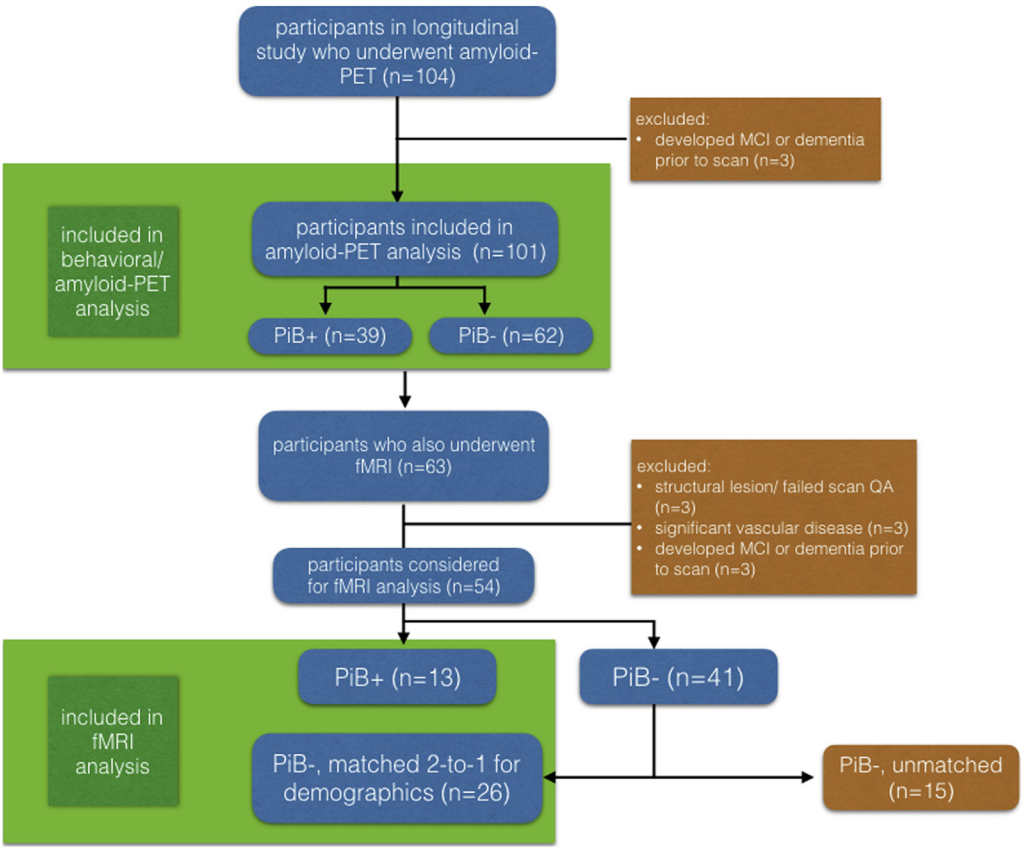

Fig. 1. Flow chart detailing subject selection for the overall analysis and imaging subset analysis. Abbreviation: PiB, [^{11}C]-Pittsburgh compound B; QA, quality assurance testing.

MRI (Philips Healthcare, The Netherlands). Each scanning session included an MP-RAGE (magnetization-prepared rapid acquisition with gradient echo) scan for anatomical imaging, with the following parameters: repetition time = 6.5 ms, echo time = 3.1 ms, slice thickness = 1.2 mm, α = 8°, 256 × 256 matrix, 170 slices, and pixel size = 1 × 1 mm^2. Each scanning session also included a T2*-weighted tf-fMRI sequence obtained over 6.1 minutes during which subjects were asked to relax with eyes open, using the following parameters: repetition time = 2000 ms, echo time = 30 ms, slice thickness = 3 mm; α = 75°, 80 × 80 matrix, 37 slices, and pixel size = 3 × 3 mm^2. Of these, 13 amyloid-positive individuals were included in the analysis based on strict exclusion criteria for head motion (no more than 3 mm of framewise motion in x/y/z or 3 degrees of motion in r/p/y dimensions; fewer than 1 in 10 repetition times showing transient motion spikes of more than 1 mm), focal imaging findings, and white matter disease. Twenty-six amyloid-negative individuals' scans, matched for demographics, served as a comparison group (Fig. 1).

2.4. PET imaging preprocessing and linear mixed models analysis

We generated parametric images of regional β-amyloid load, represented as the distribution volume ratio (DVR), using a two-compartment simplified reference tissue model with cerebellar gray matter serving as a reference region. Anatomical regions were defined using corresponding structural MRIs, as previously described [24]. The mean cortical DVR was calculated as the weighted average of values over a standard set of cortical regions. We fitted a two-class gaussian mixture model to baseline mean cortical DVR values to identify the threshold discriminating PiB-negative from PiB-positive individuals, which was determined to be 1.061, comparable to prior studies [25]. Individuals with a mean cortical DVR > 1.061 at last PiB visit were classified as PiB positive.

To avoid reliance on multiple comparisons, we used linear mixed effects models to evaluate the relationship between ultimate PiB status and longitudinal emotional reactivity and interpersonal warmth, using longitudinal emotional reactivity or interpersonal warmth as the dependent variable. Statistical analyses were conducted in SPSS 23.0 (IBM Corp, 2015) and *R* [26]. Fixed effects of the models included intercept, age, sex, PiB status, and the interactions of age, sex, and PiB status. Random effects included intercept and age. APOE ε4 gene carrier status did not contribute significantly to any effects and was removed from models. Where sex did not contribute significantly to effects, it was removed from models.

2.5. Structural imaging preprocessing and analysis

Structural MRI images were inspected for focal abnormalities, artifacts, or visible motion degradation and then analyzed for between-group differences in voxel-based morphometry using SPM12's segment program with default estimation settings and standard adult tissue probability maps (Wellcome Department of Cognitive Neurology, London; http://www.fil.ion.ucl.ac.uk/spm). Images were gray-white segmented, normalized to Montreal Neurological Institute space using default low-dimensional settings, modulated, corrected for nonlinear warping, and smoothed with an 8-mm full-width half-maximum gaussian kernel. We entered PiB-positive and PiB-negative participant maps into a second-level random effects analysis masked to the whole brain and performed two-sample t-tests to test linear contrasts between PiB-positive and PiB-negative groups. Resulting statistical parametric maps were thresholded at voxelwise thresholds of $P < .001$ (uncorrected) and $P < .05$ (FWE corrected).

2.6. Functional imaging preprocessing and analysis

Task-free fMRI scans were slice-time corrected, spatially realigned to correct for motion and measure motion parameters, coregistered to each subject's anatomical image, normalized to the Montreal Neurological Institute T1 template, smoothed with a 6-mm gaussian kernel, and temporally bandpass filtered in the frequency range of 0.008–0.15 Hz.

Resulting images were then analyzed using an unbiased, whole-brain weighted degree centrality approach to assess voxel-wise connectivity. For each subject, the blood oxygen level dependent time series for a given cortical voxel was used as a covariate of interest in a whole-brain, voxelwise linear regression, controlling for nuisance covariates for mean white matter and cerebrospinal fluid blood oxygen level dependent time series, 6 motion parameters, temporal derivatives of these 8 parameters (white matter/cerebrospinal fluid/6 motion), and squares of the resultant 16 parameters, yielding 32 nuisance parameters [27]. This resultant map of that voxel's correlation to all other cortical voxels was then spatially summed to determine that voxel's weighted whole-brain degree centrality. This process was repeated for every voxel to produce a weighted whole-brain degree map. These maps were then entered into a second-level random effects analysis masked to gray matter. We performed two-sample t-tests to evaluate linear contrasts between PiB-positive and PiB-negative groups. The resulting statistical parametric maps were thresholded using a standard joint height and extent threshold of $P < .05/0.05$ [28].

Using the thresholded maps, we selected significant clusters in the insula and superior temporal sulcus (STS) as regions of interest expected to correlate significantly with measures of emotional reactivity and interpersonal warmth. We extracted mean whole-brain degree values for each subject for each ROI and incorporated them into linear mixed models to evaluate the relationship between regional whole-brain degree and personality measures, with emotional reactivity or interpersonal warmth as the dependent variable. Fixed effects of these models included intercept, age, and whole-brain degree for STS or insula. Random effects included intercept and age. PiB status and sex did not contribute significantly to any effects and were not included.

3. Results

3.1. Participants and demographics

Participants in the larger NEO/PiB cohort were similar in handedness and years of education; more PiB-positive than PiB-negative participants were males. Because the prevalence of amyloid positivity increases with age, the amyloid-positive group was significantly older; as expected, this group also included a greater percentage of APOE ε4+ individuals. On psychometric testing, PiB-positive and PiB-negative participants scored similarly well on a measure of global cognition [29]. PiB-positive participants reported greater depressive symptoms, though their scores fell well below the clinically significant range [30], and had lower verbal episodic memory scores [31] than PiB-negative participants, though their scores, again, fell within the normal range (Table 1).

Table 1
Demographics: whole group analysis (n = 101)

Measure	PiB− (N = 62)	PiB+ (N = 39)	Normal range*	*P*	N
Age (first visit), in years, mean (SD)	63.1 (11.9)	71.4 (11.0)	n/a	<.001	101
Age (last visit), in years, mean (SD)	78.2 (8.2)	83.6 (6.6)	n/a	.001	101
Sex (% male)	46.8%	61.5%	n/a	.003	101
Handedness (% left)	6.4%	7.7%	n/a	.673	101
Years of education, mean (SD)	16.8 (2.3)	16.7 (2.1)	n/a	.722	101
APOE ε4 allele (%)	26.3%	39.5%	n/a	.003	95
MMSE, mean (SD)	28.6 (1.3)	28.4 (1.8)	≥26	.600	98
CVLT immediate, mean (SD)	55.4 (12.0)	44.8 (15.3)	24–53	.001	97
CVLT long delay, mean (SD)	12.2 (3.3)	10.0 (4.3)	3–14	.010	97
CES-D, mean (SD)	4.6 (5.9)	9.5 (8.4)	<16	.003	99

Abbreviations: APOE, apolipoprotein E; MMSE, Mini–Mental Status Examination; CVLT, California Verbal Learning Test; CES-D, Center for Epidemiologic Studies Depression Scale; SD, standard deviation.

*Global normal range for MMSE and CES-D is given. For CVLT, range given is 1 SD above and below the normative mean score for men and women aged 70–90 years.

Table 2
Demographics: subset included in fMRI analysis (n = 39)

Measure	PiB− (n = 26)	PiB+ (n = 13)	Normal range*	*P*	N
Age, in years, mean (SD)	81.2 (5.9)	83.8 (8.0)	n/a	.309	39
Sex (% male)	57.7%	61.5%	n/a	.540	39
Handedness (% left)	3.8%	15.4%	n/a	.002	39
Years of education, mean (SD)	17.0 (2.4)	16.4 (2.1)	n/a	.467	39
APOE ε4 allele (%)	26.9%	23.1%	n/a	.342	37
MMSE, mean (SD)	28.5 (1.2)	28.4 (1.9)	≥26	.793	39
CVLT immediate, mean (SD)	53.2 (13.3)	50.6 (17.2)	24–53	.641	38
CVLT long delay, mean (SD)	11.7 (4.1)	11.9 (4.2)	3–14	.888	38
CES-D, mean (SD)	5.3 (6.9)	7.6 (8.4)	<16	.398	38

Abbreviations: APOE, apolipoprotein E; MMSE, Mini–Mental Status Examination; CVLT, California Verbal Learning Test; CES-D, Center for Epidemiologic Studies Depression Scale; SD, standard deviation.

*Global normal range for MMSE and CES-D is given. For CVLT, range given is 1 SD above and below the normative mean score for men and women aged 70–90 years.

For the imaging analysis, subjects were matched for age at scan, APOE ε4 status, and other demographic variables. There were no significant between-group differences on any of these measures, with the exception of handedness (two left-handed individuals were included in the amyloid-positive group; only one appropriate amyloid-negative match was available) (Table 2).

3.2. *Amyloid-positive individuals show increasing emotional reactivity, and amyloid-positive women show a greater decline in interpersonal warmth, with age*

PiB-positive adults showed significant increases in emotional reactivity over time ($\beta = 0.49$, $t = 4.4$, $P < .001$), unlike PiB-negative participants ($\beta = -0.08$, $t = -1.0$, $P = .335$), whose scores were consistent with past studies describing a decline in neuroticism in healthy older adults [32] (Fig. 2A). There was a significant interaction between PiB status and age in determining emotional reactivity ($\beta = 0.55$, $t = 4.0$, $P < .001$), such that amyloid-positive participants showed increasing emotional reactivity with age compared with their amyloid-negative counterparts.

Although both PiB-negative ($\beta = -0.22$, $t = -4.1$, $P < .001$) and PiB-positive ($\beta = -0.29$, $t = -3.8$, $P < .001$) adults showed an overall decline in interpersonal warmth with age, consistent with past research in healthy aging samples [32], there was a significant three-way interaction between PiB status, age, and sex in determining interpersonal warmth ($\beta = 0.61$, $t = 3.3$, $P = .001$), such that there was a greater decline in PiB-positive women (Fig. 2B).

Linear mixed models were rerun in the smaller cohort included in tf-fMRI analysis to ensure that it would serve as a representative group for psychometric imaging correlations, and the same effects were observed. Specifically, we again found a significant interaction between PiB status and age on emotional reactivity ($\beta = 0.53$, $t = 3.0$, $P = .003$), as well as a significant three-way interaction between PiB, age, and sex in determining interpersonal warmth ($\beta = 0.54$, $t = 2.1$, $P = .028$).

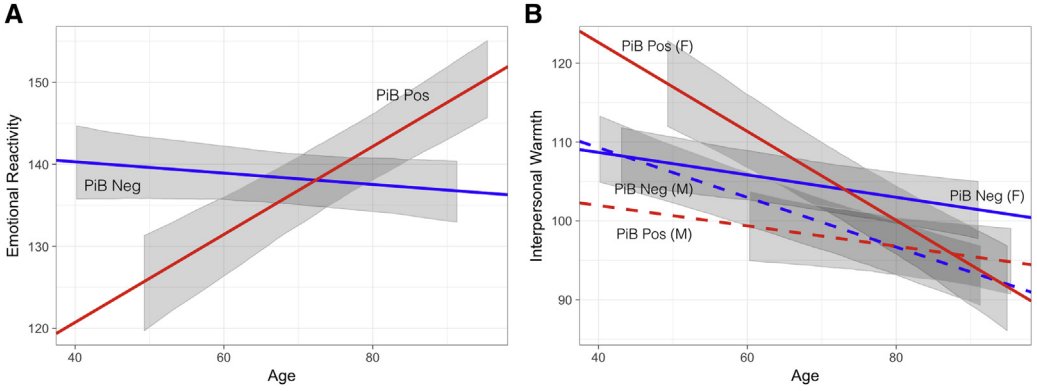

Fig. 2. Visualization of fixed effects modeling emotional reactivity and interpersonal warmth over time by amyloid status. Emotional reactivity increases longitudinally in cognitively normal PiB-positive individuals ($\beta = 0.55$, $t = 4.0$, $P < .001$) (A), whereas interpersonal warmth decreases over time in all participants, significantly more so in PiB-positive women ($\beta = 0.61$, $t = 3.3$, $P = .001$) (B). In (A), slopes are specified by the estimate of the fixed effect associated with age (for PiB-negative participants), and this fixed effect plus the fixed effect for the interaction of age by PiB positivity (for PiB-positive participants). Intercepts are specified by β_0 for the model (for PiB-negative participants), and β_0 plus the fixed effect of PiB positivity (for PiB-positive participants). (B) incorporates the fixed effect for sex and its interactions with PiB status and age to specify slopes and intercepts for PiB-negative and PiB-positive men and women. Gray ribbons represent the 95% CI of the fixed effects in the model, not incorporating residual variance or variance due to random effects, and are shown for the range of age values observed for each group. Abbreviation: PiB, [^{11}C]-Pittsburgh compound B.

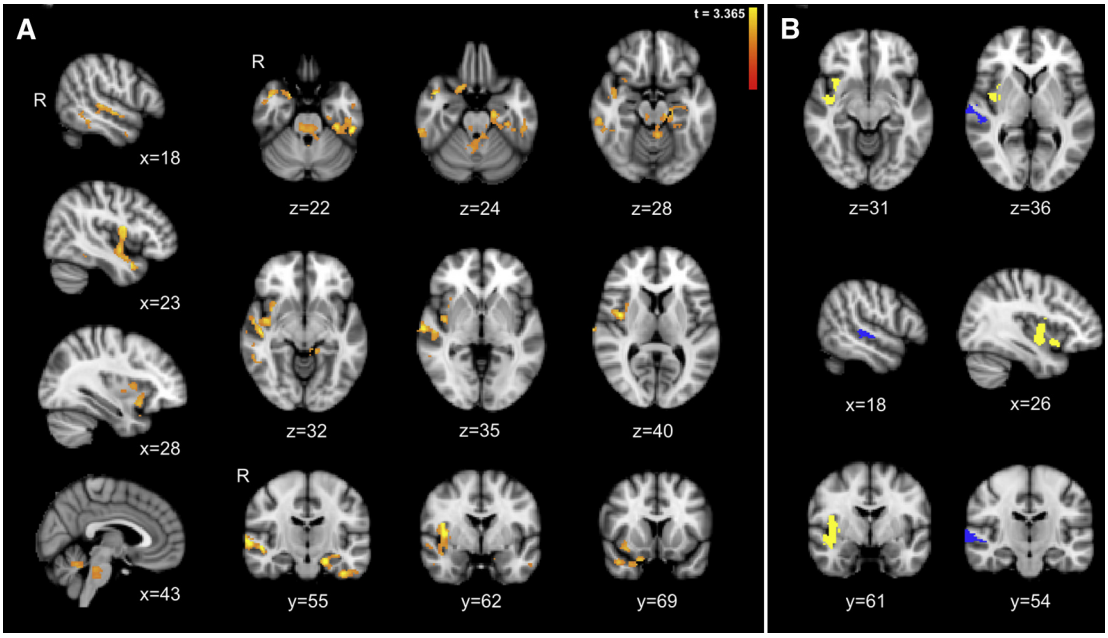

Fig. 3. Amyloid-positive individuals show increased global connectivity to the insula and superior temporal sulcus (STS). (A) Whole-brain degree analysis reveals clusters in which amyloid-positive cognitively healthy older individuals show greater global connectivity compared with matched amyloid-negative individuals, including the right insula and STS, left hippocampus and parahippocampal gyrus, temporal pole, and bilateral midbrain, midline cerebellum, and pons (including the locus coeruleus and parabrachial nucleus). There were no clusters that showed significantly lower connectivity in PiB-positive individuals. Maps are thresholded at a height by extent threshold of $P < .05/.05$. (B) We isolated the insula (yellow) and STS (blue) clusters for regional mean whole-brain degree extraction. All images are overlaid on a template MNI152 T1 2-mm brain.

3.3. Voxel-based morphometry shows no differences between amyloid-positive and amyloid-negative groups

At voxelwise thresholds of $P < .001$ (uncorrected) and $P < .05$ (FWE corrected), voxel-based morphometry assessment revealed no differences in gray matter volume between cognitively normal amyloid-positive and amyloid-negative individuals.

3.4. Amyloid-positive individuals show higher whole-brain degree centrality within insula and STS

In whole-brain degree analysis, we found significantly higher global connectivity within the right insula and STS, left hippocampus and entorhinal cortex, and bilateral midbrain and midline pons, and cerebellum in amyloid-positive older adults compared with matched amyloid-negative individuals (height by extent threshold, $P < .05$, $P < .05$; Fig. 3A).

No clusters showed significantly lower connectivity for amyloid-positive, relative to amyloid-negative healthy individuals.

3.5. Higher STS connectivity predicts lower interpersonal warmth and increased emotional reactivity

There was a main effect of STS connectivity in predicting interpersonal warmth, such that higher STS connectivity was associated with lower interpersonal warmth ($\beta = -2.8 \times 10^{-4}$, $t = -2.0$, $P = .049$) scores across participants regardless of PiB-PET status. There was a weak and opposite trend for emotional reactivity, such that higher STS connectivity was associated with increased emotional reactivity across subjects ($\beta = 3.6 \times 10^{-4}$, $t = 1.7$, $P = .106$).

There was no significant relationship between personality measures and insular connectivity.

4. Discussion

Our data show that longitudinal increases in emotional reactivity, and decreases in interpersonal warmth in women, can be detected in cognitively normal older adults with evidence of amyloid deposition. These observations build upon an emerging literature showing that adults with higher neuroticism at a single time point in midlife are at higher risk of late-onset AD [6]. The increases in emotional reactivity in PiB-positive individuals stand in contrast to older adults in general, who show decreasing neuroticism in large longitudinal studies [32].

Furthermore, we found that amyloid-positive individuals show higher global connectivity within the right anterior insula and STS, brain regions that play key roles in social processing, and that hyperconnectivity of the STS is associated with lower interpersonal warmth and a trend toward increasing emotional reactivity. Importantly, these functional changes were seen despite normal performance on cognitive tests and in the absence of structural atrophy. The right ventral anterior and mid-insula represent important

nodes within the salience network, a system critical for socially adaptive behavior [33]. The anterior insula, a hub for autonomic processing, is thought to support conscious awareness of the emotional and visceral state of the organism, based on integration of a wide variety of perceptual and interoceptive inputs [34–36]. Interestingly, the right hemisphere has been proposed as the dominant hemisphere for sympathetic autonomic processing [37–39].

The STS, a part of the posterior subnetwork of the DMN, supports key spatial and cognitive aspects of social functioning, including assessments of voice prosody, trustworthiness in faces, others' gaze, and theory of mind [40–42]. Lower STS volumes correlate with higher emotional contagion, a form of reactivity, in individuals with amnestic mild cognitive impairment and AD [3], suggesting that hyperconnectivity in the presymptomatic phase may give way to degeneration in the symptomatic phase, as proposed by some network spreading models of AD [43]. Hyperconnectivity to both insula and STS, then, could result in heightened visceral and perceptual sensitivity to salient social cues, leading to increased autonomic arousal that engenders decreased interpersonal warmth and increased emotional reactivity.

We found no regions of lower global connectivity for amyloid-positive healthy older adults compared with those without evidence of amyloid deposition. Several studies, using seed-, template-, or intrinsic component analysis–based approaches to focus analyses on structures within the DMN, have shown lower connectivity within the DMN in amyloid-positive individuals [11,13,14,44]. However, work in preclinical AD has also identified higher in-network functional connectivity from multiple DMN nodes, including a node in the middle temporal gyrus bordering the STS [11]. Other recent work demonstrates that, although the early presence of amyloid correlates with lower local connectivity within the posterior DMN, it also predicts higher connectivity from the posterior DMN to high-connectivity frontal nodes [43]. Coupled with this previous work, the current findings suggest that global hyperconnectivity from posterior division nodes of the DMN may be as important an effect of early amyloid pathology as local DMN subnetwork hypoconnectivity.

That our global, data-driven connectivity analysis did not reveal any regions of lower connectivity in amyloid-positive individuals may suggest that early amyloid-driven hypoconnectivity is restricted to local connectivity within subnetworks (i.e., the anterior or posterior DMN) in preclinical AD, while early relative hyperconnectivity to the STS, insula, and other regions (including, in our sample, the left hippocampus) may reach across subnetworks and across networks. Notably, healthy middle-aged carriers of the APOE ε4 allele show higher connectivity between salience network and DMN structures [45]. Early brainstem sites of tau deposition such as the locus coeruleus [46] would be well positioned to drive such cross-network hyperconnectivity; interestingly, we found higher global connectivity in amyloid-positive individuals in a pontine region including the locus coeruleus and the parabrachial nucleus. Parallel findings are emerging in animal research, with new data showing that transgenic amyloid-overexpressing mice have a transient period of striking DMN-like and frontocingular hyperconnectivity during midlife, which diminishes with progressive amyloid accumulation [47].

In the present study, regional STS hyperconnectivity predicted increasing emotional reactivity and decreasing interpersonal warmth, a relationship that was independent of amyloid status. Because we only assessed for amyloid near the end of longitudinal personality data included in this report, this finding raises a critical question: is insular and STS hyperconnectivity an effect of early amyloid deposition on the brain or a marker of a preexisting trait that predisposes to amyloid deposition? One theoretical model posits that individuals with preexisting hyperconnectivity may be more vulnerable to amyloid spread [43]. Conversely, in the mouse model of amyloidosis cited previously, investigators found that DMN-like and frontocingulate hyperconnectivity could be suppressed by administering antiamyloid antibodies [47], suggesting that excess amyloid accumulation is the cause of hyperconnectivity in this model. Longitudinal studies that incorporate personality and cognitive assessments with PET-amyloid and fMRI measures are ongoing and should inform this important issue in humans.

We did not find evidence for an effect of the APOE ε4 allele on emotional reactivity or interpersonal warmth in this preclinical population. Because the older average age of the cognitively healthy subjects in this study may select for ε4 carriers who are unusually resilient, our findings are not incompatible with prior studies, which have shown preclinical changes in ε4 carriers. Our findings also suggest that amyloid deposition, rather than APOE status or even clinical cognitive impairment, may be the key factor mediating personality changes in at-risk individuals. This could potentially account for the findings of a larger study in the BLSA showing that individuals later clinically diagnosed with mild cognitive impairment or AD (without amyloid testing) did not show increasing neuroticism over time compared with others [48]. To clarify these matters, future studies should examine the relationship between early amyloid deposition, the presence of an ε4 allele, and emotional reactivity in cognitively healthy individuals across the life span.

Finally, our findings run contrary to our expectations that amyloid-positive individuals would show increases in interpersonal warmth alongside increased emotional reactivity. Notably, amyloid positivity had an effect on interpersonal warmth only for amyloid-positive women, who showed higher interpersonal warmth at baseline. In individuals with higher interpersonal warmth at baseline, such as the amyloid-positive women in our sample, could increasing emotional reactivity undermine these qualities rather than enhancing them? And might higher interpersonal warmth in midlife reflect a milder, socially adaptive stage of

enhanced emotional reactivity? Further clarifying this finding could allow for the early identification of individuals who are most vulnerable to neuropsychiatric symptoms in AD.

Ongoing prevention studies are evaluating the potential efficacy of antiamyloid immunotherapy during the earliest stages of AD, with recent studies suggesting that intervention offered early enough in the disease process may lead to radiographic and potentially symptomatic improvement [49,50]. The increasing focus on preclinical AD pathophysiology highlights the importance of early identification of individuals who will go on to develop AD. Our work suggests that increasing emotional reactivity is an early and significant feature of AD, which precedes clinically appreciable cognitive symptoms or significant structural atrophy. Our data further suggest that these features may relate to higher connectivity in key cortical regions subserving social and emotional processing.

Acknowledgments

This work was supported by the Intramural Research Program of the National Institute on Aging, National Institutes of Health, USA (https://www.irp.nia.nih.gov/), and by Research and Development Contract N01-AG-3-2124.

RESEARCH IN CONTEXT

1. Systematic review: Amyloid-positivity is the first stage of preclinical Alzheimer's disease (AD). We used online databases to review the literature, which suggests that amyloid positivity is associated with characteristic changes in functional connectivity, and that changes in affect precede cognitive decline in AD. However, the longitudinal nature of emotional changes in amyloid-positive but cognitively asymptomatic individuals, and their relationship to functional connectivity, is unknown.
2. Interpretation: We show longitudinal changes in emotionality in cognitively asymptomatic individuals later found to be amyloid positive. Amyloid-positive individuals showed higher global connectivity within the right insula and superior temporal sulcus, regions that play key roles in social processing. Hyper-connectivity of the superior temporal sulcus was associated with decreasing interpersonal warmth.
3. Future directions: Future studies should use longitudinal measures of affect, amyloid positivity, and fMRI to determine whether changes in emotionality and associated hyperconnectivity in relevant regions are effects of early amyloid deposition or markers of preexisting traits that predispose to amyloid deposition.

References

[1] Guzman-Velez E, Feinstein JS, Tranel D. Feelings without memory in Alzheimer disease. Cogn Behav Neurol 2014;27:117–29.
[2] Sturm VE, McCarthy ME, Yun I, Madan A, Yuan JW, Holley SR, et al. Mutual gaze in Alzheimer's disease, frontotemporal and semantic dementia couples. Soc Cogn Affect Neurosci 2011;6:359–67.
[3] Sturm VE, Yokoyama JS, Seeley WW, Kramer JH, Miller BL, Rankin KP. Heightened emotional contagion in mild cognitive impairment and Alzheimer's disease is associated with temporal lobe degeneration. Proc Natl Acad Sci U S A 2013;110:9944–9.
[4] Benoit M, Dygai I, Migneco O, Robert PH, Bertogliati C, Darcourt J, et al. Behavioral and psychological symptoms in Alzheimer's disease. Relation between apathy and regional cerebral perfusion. Dement Geriatr Cogn Disord 1999;10:511–7.
[5] Dinzeo TJ, Sledjeski E, Durner C, Docherty NM. Comparative study of personality trait characteristics and reactivity in Schizophrenia using a film clip paradigm. Am J Psychol 2015;128:515–26.
[6] Johansson L, Guo X, Duberstein PR, Hallstrom T, Waern M, Ostling S, et al. Midlife personality and risk of Alzheimer disease and distress: a 38-year follow-up. Neurology 2014;83:1538–44.
[7] Donovan NJ, Okereke OI, Vannini P, Amariglio RE, Rentz DM, Marshall GA, et al. Association of higher cortical amyloid burden with loneliness in cognitively normal older adults. JAMA Psychiatry 2016;73:1230–7.
[8] Jansen WJ, Ossenkoppele R, Knol DL, Tijms BM, Scheltens P, Verhey FR, et al. Prevalence of cerebral amyloid pathology in persons without dementia: a meta-analysis. JAMA 2015;313:1924–38.
[9] Sperling RA, Aisen PS, Beckett LA, Bennett DA, Craft S, Fagan AM, et al. Toward defining the preclinical stages of Alzheimer's disease: recommendations from the National Institute on Aging-Alzheimer's Association workgroups on diagnostic guidelines for Alzheimer's disease. Alzheimers Dement 2011;7:280–92.
[10] Greicius MD, Srivastava G, Reiss AL, Menon V. Default-mode network activity distinguishes Alzheimer's disease from healthy aging: evidence from functional MRI. Proc Natl Acad Sci U S A 2004;101:4637–42.
[11] Mormino EC, Smiljic A, Hayenga AO, Onami SH, Greicius MD, Rabinovici GD, et al. Relationships between beta-amyloid and functional connectivity in different components of the default mode network in aging. Cereb Cortex 2011;21:2399–407.
[12] Brier MR, Thomas JB, Snyder AZ, Benzinger TL, Zhang D, Raichle ME, et al. Loss of intranetwork and internetwork resting state functional connections with Alzheimer's disease progression. J Neurosci 2012;32:8890–9.
[13] Sheline YI, Raichle ME, Snyder AZ, Morris JC, Head D, Wang S, et al. Amyloid plaques disrupt resting state default mode network connectivity in cognitively normal elderly. Biol Psychiatry 2010; 67:584–7.
[14] Hedden T, Van Dijk KR, Becker JA, Mehta A, Sperling RA, Johnson KA, et al. Disruption of functional connectivity in clinically normal older adults harboring amyloid burden. J Neurosci 2009; 29:12686–94.
[15] Zhou J, Greicius MD, Gennatas ED, Growdon ME, Jang JY, Rabinovici GD, et al. Divergent network connectivity changes in behavioural variant frontotemporal dementia and Alzheimer's disease. Brain 2010;133:1352–67.
[16] Hu WT, Wang Z, Lee VM, Trojanowski JQ, Detre JA, Grossman M. Distinct cerebral perfusion patterns in FTLD and AD. Neurology 2010;75:881–8.
[17] Rabinovici GD, Seeley WW, Kim EJ, Gorno-Tempini ML, Rascovsky K, Pagliaro TA, et al. Distinct MRI atrophy patterns in autopsy-proven Alzheimer's disease and frontotemporal lobar degeneration. Am J Alzheimers Dis Other Demen 2007;22:474–88.
[18] Balthazar ML, Pereira FR, Lopes TM, da Silva EL, Coan AC, Campos BM, et al. Neuropsychiatric symptoms in Alzheimer's disease

are related to functional connectivity alterations in the salience network. Hum Brain Mapp 2014;35:1237–46.
[19] Machulda MM, Jones DT, Vemuri P, McDade E, Avula R, Przybelski S, et al. Effect of APOE epsilon4 status on intrinsic network connectivity in cognitively normal elderly subjects. Arch Neurol 2011; 68:1131–6.
[20] Ferrucci L. The Baltimore Longitudinal Study of Aging (BLSA): a 50-year-long journey and plans for the future. J Gerontol A Biol Sci Med Sci 2008;63:1416–9.
[21] Kawas C, Gray S, Brookmeyer R, Fozard J, Zonderman A. Age-specific incidence rates of Alzheimer's disease: the Baltimore Longitudinal Study of Aging. Neurology 2000;54:2072–7.
[22] Costa PT Jr, McCrae RR. Revised NEO Personality Inventory (NEO-PI-R) and NEO Five-Factor Inventory (NEO-FFI) Professional Manual. Odessa, FL: Psychological Assessment Resources; 1992.
[23] Costa PT Jr, McCrae RR. Domains and facets: hierarchical personality assessment using the revised NEO personality inventory. J Pers Assess 1995;64:21–50.
[24] Spira AP, Gamaldo AA, An Y, Wu MN, Simonsick EM, Bilgel M, et al. Self-reported sleep and beta-amyloid deposition in community-dwelling older adults. JAMA Neurol 2013;70:1537–43.
[25] Villeneuve S, Rabinovici GD, Cohn-Sheehy BI, Madison C, Ayakta N, Ghosh PM, et al. Existing Pittsburgh Compound-B positron emission tomography thresholds are too high: statistical and pathological evaluation. Brain 2015;138:2020–33.
[26] R Development Core Team. R: A Language and Environment for Statistical Computing. Vienna, Austria: R Foundation for Statistical Computing; 2016.
[27] Satterthwaite TD, Elliott MA, Gerraty RT, Ruparel K, Loughead J, Calkins ME, et al. An improved framework for confound regression and filtering for control of motion artifact in the preprocessing of resting-state functional connectivity data. NeuroImage 2013; 64:240–56.
[28] Poline JB, Worsley KJ, Evans AC, Friston KJ. Combining spatial extent and peak intensity to test for activations in functional imaging. NeuroImage 1997;5:83–96.
[29] Folstein MF, Folstein SE, McHugh PR. "Mini-mental state". A practical method for grading the cognitive state of patients for the clinician. J Psychiatr Res 1975;12:189–98.
[30] Radloff LS. The CES-D Scale: a self-report depression scale for research in the general population. Appl Psychol Meas 1977; 1:385–401.
[31] Delis DC. CVLT-II, California Verbal Learning Test: Adult Version: Manual. San Antonio, Texas: Psychological Corporation; 1987.
[32] McCrae RR, Costa PT Jr, Pedroso de Lima M, Simoes A, Ostendorf F, Angleitner A, et al. Age differences in personality across the adult life span: parallels in five cultures. Dev Psychol 1999;35:466–77.
[33] Seeley WW, Zhou J, Kim EJ. Frontotemporal dementia: what can the behavioral variant teach us about human brain organization? Neuroscientist 2012;18:373–85.
[34] Critchley HD, Rotshtein P, Nagai Y, O'Doherty J, Mathias CJ, Dolan RJ. Activity in the human brain predicting differential heart rate responses to emotional facial expressions. NeuroImage 2005; 24:751–62.
[35] Critchley HD, Melmed RN, Featherstone E, Mathias CJ, Dolan RJ. Volitional control of autonomic arousal: a functional magnetic resonance study. NeuroImage 2002;16:909–19.
[36] Seeley WW, Allman JM, Carlin DA, Crawford RK, Macedo MN, Greicius MD, et al. Divergent social functioning in behavioral variant frontotemporal dementia and Alzheimer disease: reciprocal networks and neuronal evolution. Alzheimer Dis Assoc Disord 2007;21:S50–7.
[37] Oppenheimer SM, Gelb A, Girvin JP, Hachinski VC. Cardiovascular effects of human insular cortex stimulation. Neurology 1992; 42:1727–32.
[38] Yoon BW, Morillo CA, Cechetto DF, Hachinski V. Cerebral hemispheric lateralization in cardiac autonomic control. Arch Neurol 1997;54:741–4.
[39] Colivicchi F, Bassi A, Santini M, Caltagirone C. Cardiac autonomic derangement and arrhythmias in right-sided stroke with insular involvement. Stroke 2004;35:2094–8.
[40] Hoffman EA, Haxby JV. Distinct representations of eye gaze and identity in the distributed human neural system for face perception. Nat Neurosci 2000;3:80–4.
[41] Narumoto J, Okada T, Sadato N, Fukui K, Yonekura Y. Attention to emotion modulates fMRI activity in human right superior temporal sulcus. Brain Res Cogn Brain Res 2001;12:225–31.
[42] Pelphrey KA, Morris JP, McCarthy G. Grasping the intentions of others: the perceived intentionality of an action influences activity in the superior temporal sulcus during social perception. J Cogn Neurosci 2004;16:1706–16.
[43] Jones DT, Knopman DS, Gunter JL, Graff-Radford J, Vemuri P, Boeve BF, et al. Cascading network failure across the Alzheimer's disease spectrum. Brain 2016;139:547–62.
[44] Buckley RF, Schultz AP, Hedden T, Papp KV, Hanseeuw BJ, Marshall G, et al. Functional network integrity presages cognitive decline in preclinical Alzheimer disease. Neurology 2017;89:29–37.
[45] Goveas JS, Xie C, Chen G, Li W, Ward BD, Franczak MB, et al. Functional network endophenotypes unravel the effects of apolipoprotein E epsilon 4 in middle-aged adults. PLoS One 2013;8:e55902.
[46] Braak H, Thal DR, Ghebremedhin E, Del Tredici K. Stages of the pathologic process in Alzheimer disease: age categories from 1 to 100 years. J Neuropathol Exp Neurol 2011;70:960–9.
[47] Shah D, Praet J, Latif Hernandez A, Hofling C, Anckaerts C, Bard F, et al. Early pathologic amyloid induces hypersynchrony of BOLD resting-state networks in transgenic mice and provides an early therapeutic window before amyloid plaque deposition. Alzheimers Dement 2016;12:964–76.
[48] Terracciano A, An Y, Sutin AR, Thambisetty M, Resnick SM. Personality change in the preclinical phase of Alzheimer disease. JAMA Psychiatry 2017;74:1259–65.
[49] Sevigny J, Chiao P, Bussiere T, Weinreb PH, Williams L, Maier M, et al. The antibody aducanumab reduces Aβ plaques in Alzheimer's disease. Nature 2016;537:50–6.
[50] Siemers ER, Sundell KL, Carlson C, Case M, Sethuraman G, Liu-Seifert H, et al. Phase 3 solanezumab trials: secondary outcomes in mild Alzheimer's disease patients. Alzheimers Dement 2016;12:110–20.